Orig Life Evol Biosph (2016) 46:149–169
DOI 10.1007/s11084-015-9468-8

PREBIOTIC CHEMISTRY

# Chemical Analysis of a "Miller-Type" Complex Prebiotic Broth

## Part I: Chemical Diversity, Oxygen and Nitrogen Based Polymers

**Eva Wollrab[1,6] · Sabrina Scherer[1] · Frédéric Aubriet[2] · Vincent Carré[2] · Teresa Carlomagno[3,4,5] · Luca Codutti[3,5] · Albrecht Ott[1]**

Received: 29 May 2015 / Accepted: 27 August 2015 /
Published online: 27 October 2015


**Abstract** In a famous experiment Stanley Miller showed that a large number of organic substances can emerge from sparking a mixture of methane, ammonia and hydrogen in the presence of water (Miller, Science 117:528–529, 1953). Among these substances Miller identified different amino acids, and he concluded that prebiotic events may well have produced many of Life's molecular building blocks. There have been many variants of the original experiment since, including different gas mixtures (Miller, J Am Chem Soc 77:2351–2361, 1955; Oró, Nature 197:862–867, 1963; Schlesinger and Miller, J Mol Evol 19:376–382, 1983; Miyakawa et al., Proc Natl Acad Sci 99:14,628–14,631, 2002). Recently

**Electronic supplementary material** The online version of this article (doi:10.1007/s11084-015-9468-8) contains supplementary material, which is available to authorized users.

✉ Eva Wollrab
eva.wollrab@physik.uni-saarland.de

Albrecht Ott
albrecht.ott@physik.uni-saarland.de

[1] Biologische Experimentalphysik, Universität des Saarlandes, Campus, Geb. B2 1, 66123 Saarbrücken, Germany

[2] Laboratoire de Chimie et Physique Multi-échelle des Milieux Complexes (LCP-A2MC), Université de Lorraine, 1 Boulevard Arago, 57078 Metz, France

[3] Structural and Computational Biology Unit, European Molecular Biology Laboratory, Meyerhofstraße 1, 69117 Heidelberg, Germany

[4] Helmoltz Zentrum für Infektionsforschung, Inhoffenstraße 7, 38124 Braunschweig, Germany

[5] Centre of Biomolecular Drug Research, Leibniz University, Schneiderberg 38, 30167 Hannover, Germany

[6] Present address: Laboratory of Microbial Morphogenesis and Growth, Institut Pasteur, 75724 Paris Cedex 15, France

some of Miller's remaining original samples were analyzed with modern equipment (Johnson et al. Science 322:404–404, 2008; Parker et al. Proc Natl Acad Sci 108:5526–5531, 2011) and a total of 23 racemic amino acids were identified. To give an overview of the chemical variety of a possible prebiotic broth, here we analyze a "Miller type" experiment using state of the art mass spectrometry and NMR spectroscopy. We identify substances of a wide range of saturation, which can be hydrophilic, hydrophobic or amphiphilic in nature. Often the molecules contain heteroatoms, with amines and amides being prominent classes of molecule. In some samples we detect ethylene glycol based polymers. Their formation in water requires the presence of a catalyst. Contrary to expectations, we cannot identify any preferred reaction product. The capacity to spontaneously produce this extremely high degree of molecular variety in a very simple experiment is a remarkable feature of organic chemistry and possibly prerequisite for Life to emerge. It remains a future task to uncover how dedicated, organized chemical reaction pathways may have arisen from this degree of complexity.

**Keywords** Origin to life · Complex chemical mixture · Mass spectrometry · NMR · Miller-Urey experiment

## Introduction

In 1953 Stanley Miller showed that biomolecules can emerge spontaneously from water, methane, hydrogen and ammonia (Miller 1953). In the experiment electrodes discharged electricity in a gas mixture that cycles above a water reservoir in a closed environment. After several days Miller detected different organic molecules in the emerging broth, amino acids among them. Miller concluded that biomolecules may have formed spontaneously on the early Earth as a first step towards Life.

Among the prominent substances directly produced from the gas mixture by the discharge are HCN as well as aldehydes (Miller 1955). These are known to form amino acids following Strecker synthesis. HCN is also known to polymerize to give adenine (Miller 1957; Oró 1960). In water, concentrated HCN alone combines to produce many different types of polymers among other complex structures, some of them insoluble (Ruiz-Bermejo et al. 2012; Bonnet et al. 2013). Due to its suspected role in the origin of Life this complex matter has been investigated in great detail (He et al. 2012; Matthews and Minard 2006; Matthews 1975; Ferris and Hagan 1984).

Many objected to Miller's experiment that the atmosphere of the early Earth was unlikely to have been similarly reducing when Life emerged (Miyakawa et al. 2002; Shaw 2008). Recently, Cleaves et al. (2008) showed that significant amounts of amino acids can be produced under neutral conditions and if oxidation inhibitors (e.g. vitamin C, ferrous iron) are present to prevent their degradation in the broth. Miller's experiment inspired many more investigations. In Miller-type experiments amino acids and amines were produced from sparking various gas mixtures (Sanchez et al. 1966b; Oró 1963; Parker et al. 2011). Different energy sources such as high-energy particles (Kobayashi et al. 1998), UV irradiation (Santamaria and Fleischmann 1966) or thermal energy (Fox 1995) were also able to produce amino acids from gaseous precursors or small organic compounds (Oró et al. 1959; Lowe et al. 1963). Besides amino acids, other biomolecules, not found in Miller's initial experiments, such as nucleobases (Lowe et al. 1963; Sanchez et al. 1966a; Oró 1960; Ferus et al. 2014) or lipids (Lowe et al. 1963; McCollom et al. 1999) can form from small organic compounds and polymerize under possible prebiotic conditions (Trinks et al. 2005; Simionescu

et al. 1976). We understand that if the required simple molecular building blocks are rapidly quenched from a highly excited state under reducing conditions, they statistically combine to different larger molecular structures, some of which play important roles in today's organisms.

Many studies have been performed to detect the presence of biomolecules in prebiotic mixtures, and many chemical pathways that led to their formation have been discovered (Oró 1961; Miller 1957; Tian et al. 2011; Matthews and Minard 2006). This research was performed when analytical technology was not as advanced as it is now. In analytical experiments usually highly selective techniques such a chromatography were employed to isolate the component of interest. Here we took the opposite route and analyzed the components without preselection. We used mass spectrometry and NMR (Nuclear Magnetic Resonance). The degree of complexity of the studied molecular mixture poses an analytical challenge. Often, related substances broaden the signals complicating the identification of substances. NMR signal intensity is a known function of concentration, and this enables to determine functional groups of the substances quantitatively. Since NMR measurements can take days, they necessarily provide information about the equilibrated mixture.

Mass spectrometry is a very sensitive and fast technique. Different ionization modes (positive or negative) and the ESI technique (electrospray ionization) emphasize different subsets of the mixture. In many cases, fragmentation measurements enable access to the chemical structure of the molecules. High-resolution mass spectrometry is able to resolve even complex mixtures, and no prior chromatographic selection is required.

The comprehensive chemical analysis provides a global view on the ingredients enabling a more statistical analytical approach. We consider this an elementary first step in the quest to understand the reaction-dynamics that led to early Life.

## Methods

### Experimental Procedure

We studied different variants of the original Miller-Urey experiments (Miller 1953, 1955). In set-up I a 5 l flask with two tungsten electrodes sat on top of a 1 l flask filled with deionized water (Sartorius stedim biotech, arium 611UV or GENO, Grünbeck) (Fig. 1a)). The water was heated. A high-voltage device (home-made, based upon a transformer from a cathode ray tube, max. 25 kV) produced sparks in the gas phase (∼10 kV sawtooth, 20 Hz, ∼20 W, direct current). A stop-cock enabled the evacuation and filling of the reactor. We extracted samples via a capillary. Set-up II differed in that the sparking took place between one electrode and the surface of the mixture, grounded by a second electrode (Fig. 1b)).

We evacuated and immediately refilled the glass apparatus with methane several times to reduce contamination by atmospheric gases to the amount dissolved in the water. Degassing the water as well as the order of filling the gases had no detectable influence on the observed mass spectra. We then injected the gases methane (purity 2.5, Praxair), ammonia (purity 3.8, Praxair) and hydrogen (purity 3.0, Praxair). We heated up the experiment to a temperature between 90–100 °C that we kept constant during the experimental run. We varied the amount of methane in the range of 40–78 %, ammonia 22–40 % and hydrogen 0–20 %. After filling the apparatus with the gas mixture (initial pressure about 0.9 atm) we started the electrical sparking. The pressure in a running experiment was about 1.1 atm, about constant until the end of the experiment. We kept the experiments running for one or two days.

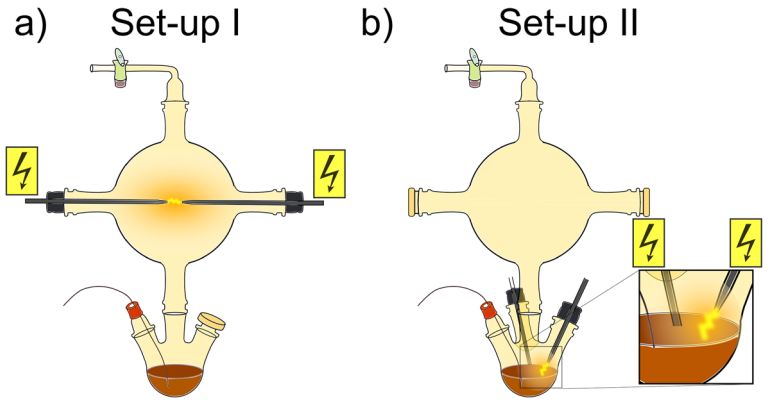


**Fig. 1** Experimental variants of the original Miller-Urey experiment (Miller 1953). **a** In set-up I sparking takes place in the gas phase between two electrodes. **b** In set-up II sparking occurs between the electrode and the liquid surface

We did not refill any of the gases. In some experiments we added phophoric acid to the deionized water.

If extracted samples could not be analyzed directly, we immediately lyophilized or froze them for further analysis. We did not observe any changes in the mass spectra due to lyophilization, even after storage for several months. Frozen samples were analyzed after a few days.

## Analytical Techniques

All samples were analyzed by Q-Tof mass spectrometry. For further analysis we employed high-resolution mass spectrometry and NMR.

### *Q-Tof Mass Spectrometry*

All samples were routinely analyzed in a quadrupole time-of-flight mass spectrometer (Q-Tof MS), equipped with electrospray ionization (ESI) (Micromass Q-Tof micro, MS Vision). Prior to analysis we diluted the samples by a mixture of acetonitrile (Carl Roth, Rotisolv $\geq$ 99.95 %) and deionized water (1:1) by a factor of 100. In the positive ionization mode (ESI+), molecules were observed as pseudo molecular ions with $H^+$, $NH_4^+$, $Na^+$ or $K^+$ adducts, which derived from the glassware or the atmosphere, and maybe a weak contribution from the solvent (Greig and Griffey 1995). In the negative ionization mode (ESI-) molecules ionized by releasing a proton. Hence ESI-MS is sensitive to polar molecules that can be charged easily. ESI is a "soft" ionization technique and analytes generally stay intact during this process (Watson and Sparkman 2008). Small molecules as those observed here are generally singly charged (Gross 2011). Besides concentration, the intensity in a mass spectrum is a function of the ionizability of a substance, as well as the molecular environment. As a result mass spectrometry without coupling to chromatography does not enable quantification of concentrations easily.

The quadrupole can be used to filter a certain mass range. In our measurements we adjusted it to transfer molecules between m/z 50 to 1000 during one scan. The m/z ratio was determined by time of flight measurements where we set the scan time to 1.0 s with an inter scan time of 0.1 s. The nominal resolution of the instrument is 5000 FWHM. The instrument provided a fast, on-site method to obtain a fingerprint of the samples.

*FTICR MS*

We performed high-resolution mass spectrometry on a Fourier Transform Ion Cyclotron Resonance (FTICR) mass spectrometer (910-MS FTMS, Varian, 9.4 T) equipped with ESI (electrospray ionization) or LDI (laser desorption ionization) in positive and negative ion mode. In LDI a laser beam (355 nm) irradiates the sample and induces the desorption/ionization of the molecule. Fragmentations can occur in this ionization method. The high resolution (350,000 FWHM at m/z 250) of the instrument enabled us to analyze the complex mixture without prior chromatography. We optimized ion transfer with respect to the mass range of interest. To increase the signal, we accumulated ions during a few minutes. We calibrated the mass spectrometer externally with a standard solution. Internal calibration was performed with Omega 8 software (Varian-Ion Spec Inc.) to an accuracy of about 1 ppm.

The instrument provided the option of high-resolution tandem mass spectrometry (MS/MS). For this, ions were accumulated and selected in the spectrometer cell before ions of a specified mass-charge ratio were accelerated to collide with nitrogen gas. This led to fragmentation of the ions (SORI-CID). The characteristic fragmentation pattern gives information about the chemical structure.

*NMR*

We solubilized the lyophilized samples in deuterated PBS buffer (150 mM NaCl, pH 7.4) and immediately analyzed them by NMR (Avance II, Bruker, 290 K, 800 and 600 MHz, cryoprobe and triple resonance probe). We recorded homonuclear 2D spectra, such as stimulated-echo and LED corrected DOSY (Wu et al. 1995), COSY (Piantini et al. 1982) and ROESY (Bothner-By et al. 1984) (mixing time, 400 ms), and heteronuclear correlations, such as $^{13}$C-HMQC (Bax et al. 1983) and HMBC (Bax and Summers 1986). For one sample we recorded a 50 ms TOCSY (Braunschweiler and Ernst 1983) experiment as well.

We acquired DQF-COSY and ROESY with 96 scans, 256 increments in $t_1$ and a sweep-width of 12 ppm; $^{13}$C-HMQC and HMBC were recorded with 80–256 scans, 128 increments in $t_1$ and $^{13}$C sweep-widths of 70 and 230 ppm, respectively.

We calibrated DOSY experiments using a mixture of molecules with molecular weights between 200 to 2000 Da; the optimized values for $\Delta$ and $\delta$ delays were 50 and 4.6 ms respectively. The final DOSY analysis was based on a set of 16 1D experiments recorded with 256 scans each, ramping the gradient strength from 2 to 95 %. Spectra were processed and analyzed using both Bruker Topspin 3.0 and MestReLab MNova NMR(Willcott 2009).

*pH*

Throughout the experiment we could monitor the pH value by continuously pumping small amounts of the solution through a flow chamber (in-house fabrication) with a pH electrode (Lazar Research Laboratories, Inc.) suitable for microliter volumes.

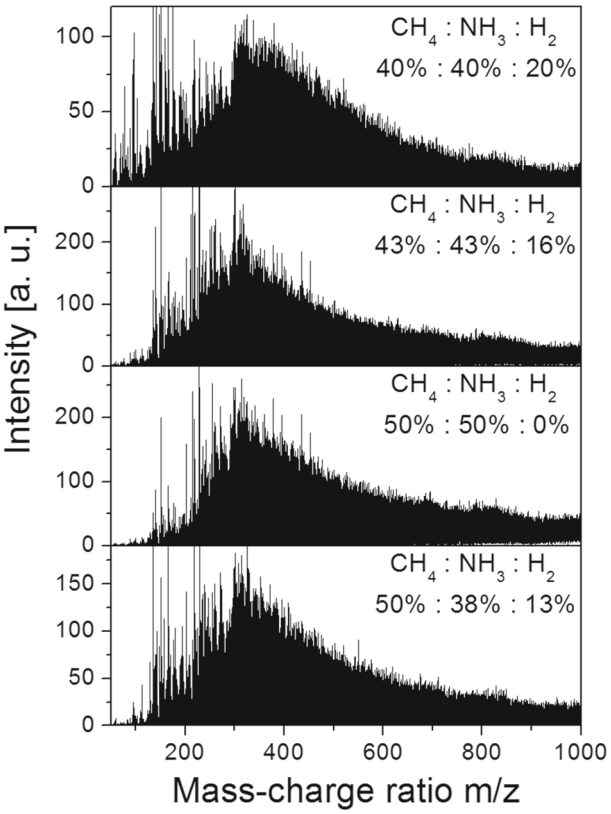


**Fig. 2** Mass spectra from samples extracted from the Miller-Urey experiment (set-up I) running for about 22 h. For comparative scaling a few peaks of high intensity are cropped. Different spectra correspond to different initial gas mixtures, but their bulk spectra are nevertheless quite similar

*SEM*

Solid particles from the solution of the Miller-Urey experiment were deposited on a silicon wafer for scanning electron microscope (SEM) measurements. SEM was performed on a JEOL JSM-7000 F at 20 kV equipped for energy-dispersive X-ray spectroscopy (EDS).

## Results

We reduced the amount of hydrogen compared to the original experiment ($CH_4$:$NH_3$:$H_2$ of 40 %:40 %:20 %) to investigate its influence on the resulting substances. We observed only little changes (Fig. 2), confirming Miller's finding that omitting hydrogen had no effect on the results (Miller 1955). Running times longer than about two days did not lead to a noticeable change in mass spectrum. The addition of phosphoric acid had no detectable influence on the composition of the mixture.

We found solid particles in the samples. Beside grains of tungsten we observed mostly organic filamentous structures (Fig. 3).

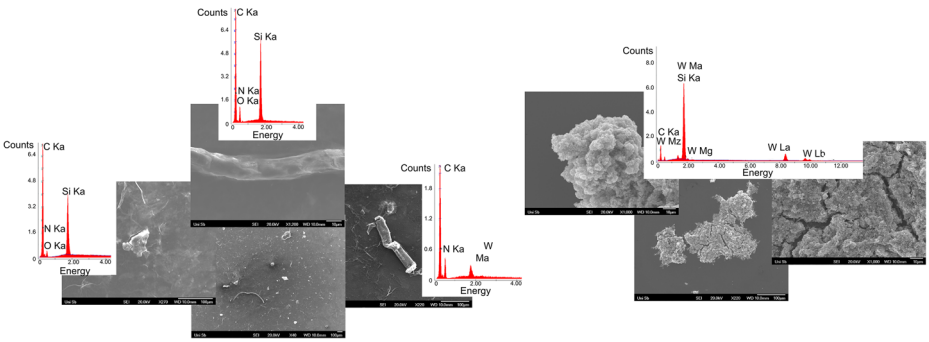


**Fig. 3** SEM images with corresponding EDS analysis of solid particles in the sample. We found different solid structures in the mixture (set-up II). The filamentous structures are mostly organic whereas the porous grains correspond to tungsten compounds. The silicon signal is due to the silicon wafer used

## High-Resolution Mass Spectrometry - ESI FTICR MS Measurements

In the ESI+ Q-Tof mass spectra we observed masses in 150 to 1000 m/z range. The shape of the mass distribution was independent of the gas composition. We aimed at identifying small molecules because we assumed that they were early products in the experiment, and they were the building blocks of the larger molecules. Accordingly, we adjusted the ion transfer to the range m/z 150 to 300.

### *Mass Spectra*

Since we obtained very similar results for other studied samples, in the following we limit our discussion to the analysis of a typical sample, taken from set-up I and studied using ESI FTICR. Before sample extraction the experiment ran for about 5 days ($CH_4$:$NH_3$:$H_2$ 2:2:1). In the mass spectra from the ESI+ and ESI- measurements we identified 668 substances (Fig. 4, Supplementary Table 1). Three hundred forty-seven substances appeared in ESI+ mode, measurements with a mean error of $-0.035\pm0.656$ ppm, and 487 substances in the ESI- measurements with a mean error of $-0.042\pm0.391$ ppm. One hundred sixty-six substances were common to both ion modes. In the negative ion mode we identified several tungsten species, the most prominent peak from tungsten oxide $WO_3OH^-$ (m/z 248.93896). In the positive ion mode we identified the most intense species as $C_8H_{13}O_4^+$ (m/z 173.08084), which can be assigned to different protonated carboxylic acids and esters [$C_8H_{12}O_4 + H^+$].

Due to the large amount of substances present in this mass range, we derived chemical indices and used graphical analysis tools as post acquisition data treatment to ensure an easier interpretation of the results. This enabled us to estimate the amount of double bonds and aromatic rings. By plotting the data points in different diagrams that have been proposed in the literature, we highlighted characteristics and identified chemical classes of molecules.

### *Chemical Indices*

High-resolution mass spectrometry directly delivered the molecular formulas of the detected substances. We find that an average detected molecule was composed of $34.89\pm6.68$ % carbon, $37.25\pm9.82$ % hydrogen, $18.86\pm9.77$ % nitrogen and $9.04\pm7.20$ % oxygen (e.g.

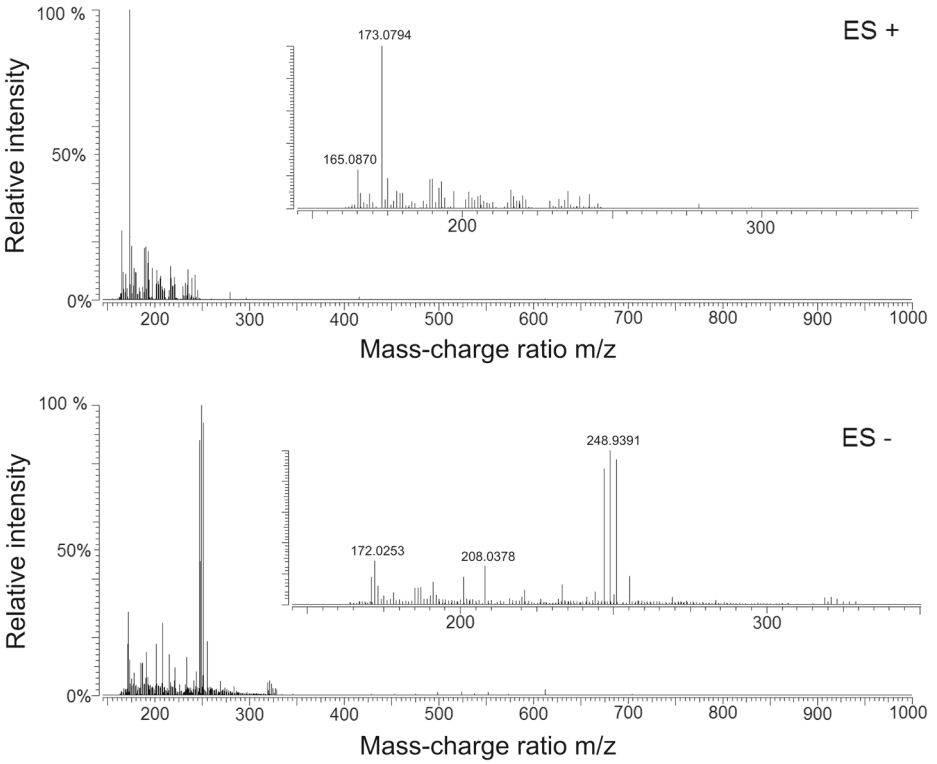


**Fig. 4** ESI FTICR mass spectrum of a sample from the Miller-Urey experiment (set-up I, $CH_4$:$NH_3$:$H_2$ 2:2:1) 123 h after the start of the experiment in the positive and negative ion mode. We adjusted the ion transfer to the range m/z 150 to 300. The strongest signals are from $C_8H_{13}O_4^+$ (ESI+) and $WO_3OH^-$ (ESI-)

$C_7H_7N_3O_2$, corresponding to 2,6-Pyridine Dicarboxamide). Since ESI-MS is not a quantitative technique we did not weight the atomic fraction with intensities to obtain these values.

The double bond equivalent (DBE) corresponds to the number of double bonds and rings in an organic molecule composed of carbon, hydrogen, nitrogen and oxygen (Gross 2011; Watson and Sparkman 2008).

$$DBE = 1 + c + \frac{n - h}{2}, \quad c, h, n \text{ - number of C, H, N atoms} \tag{1}$$

To analyze the degree of saturation, we determined the DBE for each substance in the sample. We find that the mean number of rings and double bonds is 7.2 with a standard deviation of 2.9 (Fig. 5). For every mass range we find a broad distribution of degrees of saturation.

The aromaticity index (AI) measures the density of double bonds between carbon atoms in a molecule (Koch and Dittmar 2006). For molecules with a large number of heteroatoms the AI would turn negative in which case it is defined as zero to keep the notion of a density. This index explicitly considers oxygen atoms in the calculation.

$$AI = \max\left[\frac{1 + c - o - \frac{h}{2}}{c - o - n}, 0\right] \tag{2}$$

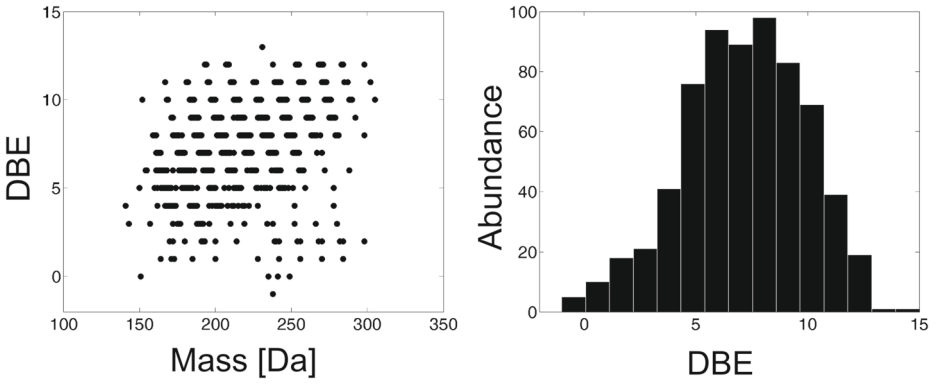


**Fig. 5** Scatter plot of DBE by mass and distribution of DBE derived from ESI± FTICR measurements (mass spectra in Fig. 4). The plots correspond to 99.3 % of the substances observed. For every mass range we find a broad distribution of DBEs

Molecules with an AI > 0.5 are considered to contain at least one aromatic ring, molecules with AI ≥ 0.67 are considered as polyaromatic species (Koch and Dittmar 2006). For our sample the mean AI is 0.98 with a standard deviation of 1.38. 44.9 % of the substances present an AI of zero due to the large amount of heteroatoms. We find that statistically

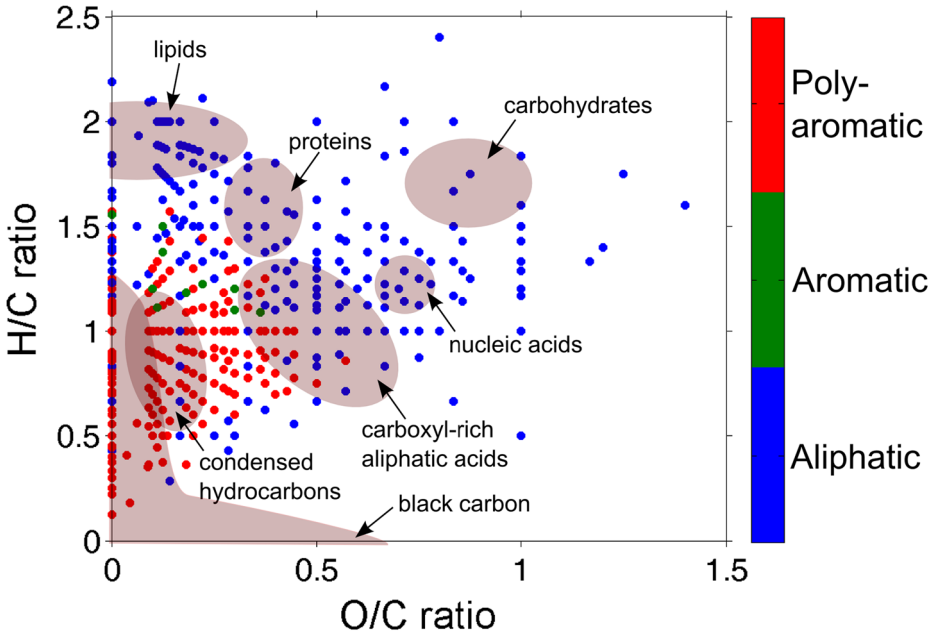


**Fig. 6** Van Krevelen diagram from a measurement in ESI± FTICR MS (mass spectra in Fig. 4). Hydrogen/carbon ratio as a function of the oxygen/carbon ratio (H/C and O/C) for 99.4 % of the observed substances. Substances are heuristically classified into aromaticity as calculated from the AI. Molecules on vertical lines differ by their amount of hydrogen. Regions of the diagram that correspond to specific classes of molecules (Kim et al. 2003a; Hertkorn et al. 2008) are highlighted and annotated

46.0 % of the molecules contain at least one aromatic ring while 44.2 % of the molecules statistically contain several condensed aromatic rings.

*Van Krevelen Diagrams and Kendrick Maps*

Van Krevelen diagrams are current data processing tools used in high-resolution MS to classify detected chemical substances (Gross 2011; Kim et al. 2003a; Schramm et al. 2011; Reemtsma 2009). In these diagrams the atomic ratio of hydrogen/carbon is assigned to the y-axis and the ratio of oxygen/carbon or nitrogen/carbon is assigned to the x-axis.

We plot the ESI± FTICR data of our sample in Van Krevelen diagrams (Figs. 6 and 7). Most of the molecules show an O/C and N/C ratio between 0 and 1 and a H/C ratio between 0 and 2. For completely saturated alkanes the latter ratio is slightly above 2. The diagrams highlight that molecules are either very unsaturated, containing many double bonds and aromatic rings, or they contain an important number of heteroatoms.

From the position of different classes of organic molecules in the Van Krevelen diagram (Fig. 6) we see that the Miller-Urey experiment creates a wide spectrum of organic molecules.

Kendrick maps are another illustration of mass spectrometry data, widely used in the analysis of complex chemical mixtures (Kendrick 1963; Schramm et al. 2011; Hertkorn et al. 2008). For plotting Kendrick maps a certain motif (e.g. $CH_2$) is chosen to define the exact integer mass (e.g. 14.00 units whereas its mass in the IUPAC system is 14.01565 Da). Masses of the IUPAC system $m_{IUPAC}$ are transformed to Kendrick masses $m_K = m_{IUPAC} \cdot \frac{14}{14.01565}$ and the Kendrick mass defect is calculated $KMD = m_n - m_K$, where $m_n$ is the nominal mass of the molecule. After the transformation, the members of homologous series (e.g. $(CH_2)_n$) of the respective motif lie on a horizontal line and are easy to identify.

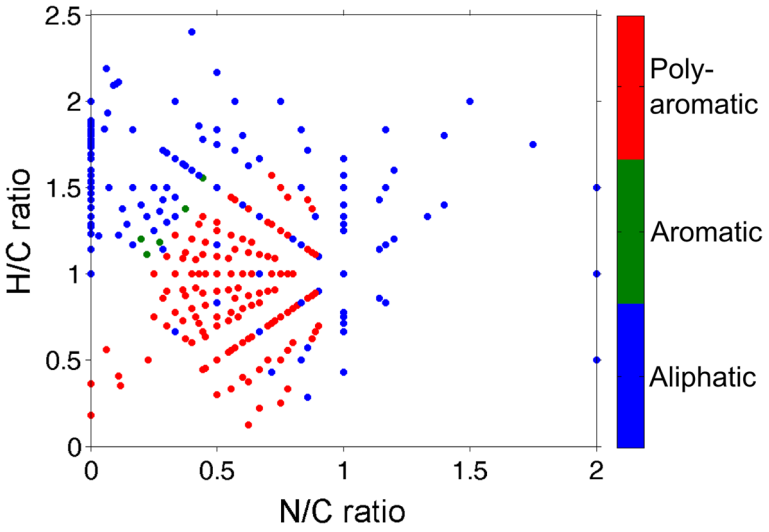


**Fig. 7** Van Krevelen diagram of the sample measured in ESI± FTICR MS (mass spectra in Fig. 4). Hydrogen/carbon ratio as a function of the nitrogen/carbon ratio (H/C and N/C) for 99.4 % of the observed substances. *Colors* indicate aromaticity from the AI

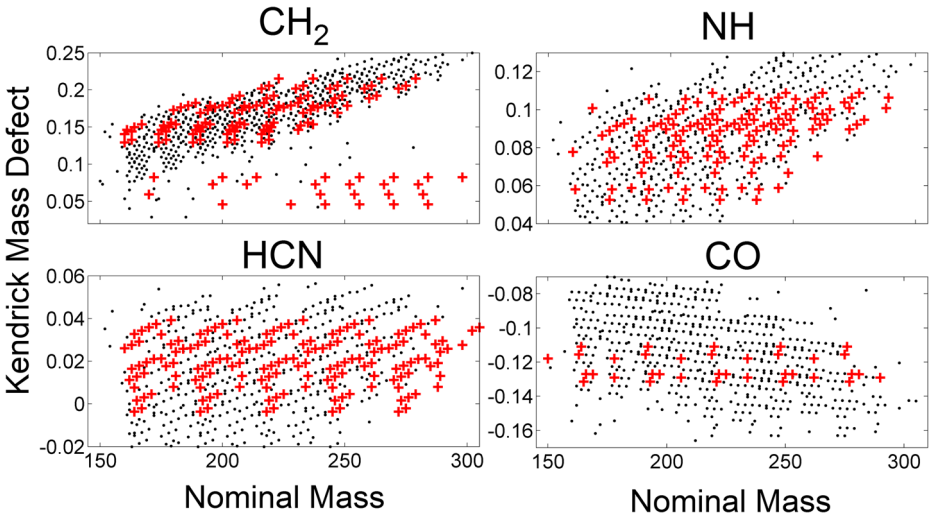


**Fig. 8** Kendrick maps from the sample measured in ESI± FTICR MS (mass spectra in Fig. 4). We tested different motifs as base masses to identify possible homologous series. The motifs $CH_2$, NH, HCN and CO give rise to the largest groups of homologous series. The *red crosses* indicate series of a motif with at least 5 members. The data points correspond to around 90 % of the identified substances, the others are outside the range of the diagrams

We tested for all motifs of the type $C_{0-9}H_{0-21}N_{0-9}O_{0-9}$. We plot Kendrick maps for the different motifs and identify several series (Fig. 8). The motifs $CH_2$, NH, HCN and CO give rise to the largest groups of homologous series (highlighted in red).

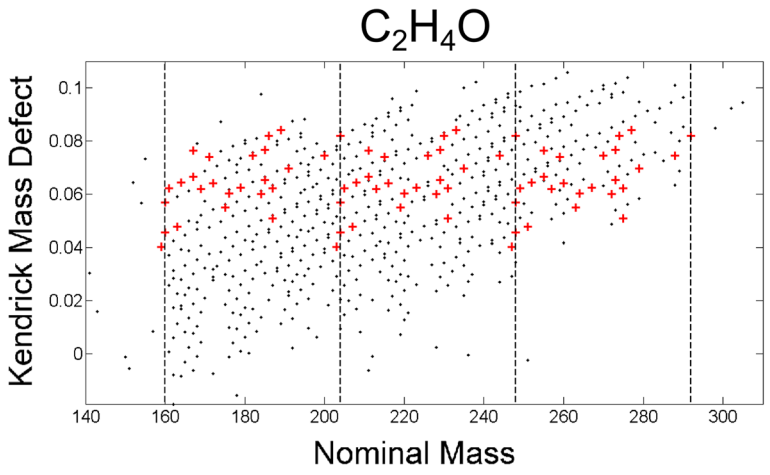


**Fig. 9** Kendrick maps from a typical sample from the Miller-Urey experiment measured in ESI± FTICR MS (mass spectra in Fig. 4). We find several three-membered homologous series of $C_2H_4O$ (*red crosses*), pointing towards the addition of several ethylene glycols. The *vertical lines* indicate a distance of 44 Da (nominal mass of $C_2H_4O$). The depicted data points correspond to around 91.8 % of the identified substances. The others are off scale

*Identification of Polymeric Species*

In the Kendrick map based on $C_2H_4O$ (44.02621 Da), several series are visible (Fig. 9). Each series consists of three members stretching over the whole measured mass range (about 150 – 300 Da). For some samples in the ESI+ Q-Tof mass spectra, we observed intense series of equidistant peaks (distance m/z 44.04±0.04), pointing towards the existence of oligomers. The resolution of the instrument does not enable unambiguous identification of one or more monomers. Accordingly, we analyzed one of the corresponding samples (78 % $CH_4$, 22 % $NH_3$, set-up II, 50 nM phosphoric acid) in the FTICR mass spectrometer with ESI and LDI ionization techniques in the positive ion mode. To obtain an increased signal, we adjusted the ion transfer to a mass range of m/z 200 to 600. Generally we detected protonated ions but we also found cationization by $Na^+$, $NH_4^+$ and $K^+$ (less abundant).

Taking all observations together we find 12 different trains of peaks in the sample. The trains correspond to different polymers that are composed of the same monomers. The ESI Q-Tof instrument detected most of them as well (Table 1). The high-resolution instrument clearly showed that all oligomers stem from monomers of chemical formula $C_2H_4O$ suggesting polyethylene glycol (PEG) species. Some trains II–VI only differ by a single $CH_2$, pointing to alkyl groups. The oligomers comprise only few or no nitrogen atoms.

For structure analysis by ESI FTICR MS/MS, we considered four oligomers that prominently appear in the ESI+ spectra. The fragmentation patterns (Supplementary Table 2) reveal typical PEG fragmentation (Lattimer 1992a, b; Kalinoski and Hargiss 1992; Selby et al. 1994). Chains of PEG of different lengths are attached to an alkane chain of $(CH_2)_{11}$ and there is no mixing between the PEG monomers and units of $CH_2$. Indeed the main fragment loss corresponds to an oligomer of PEG. PEG is a frequent contaminant in mass spectrometry, however, we believe this not to be the case. Our samples were not in contact with any other surfaces but clean glass, PTFE and PEEK. The entire experimental setup was thoroughly cleaned before each experimental run. We only detected PEG in experiments that had been already running for at least a night. PEG did not emerge during the Q-TOF analysis, since PEG free samples and PEG containing samples are immediately distinguished in repetitive measurements in the same instrument, and the same PEGs appeared in different instruments equipped with different sources for ionization. The PEG we observe in the experiment is not a standard contaminant but exhibits a hydrophobic alkane tail.

We can only attribute a small number of mass peaks to substances that do not belong to a series of PEG polymers (26 % for ESI+ and 16 % for LDI). We find these substances in the mass range of about m/z 350 to 700 (Supplementary Table 3).

## NMR

Prior to the NMR measurement we fractionated the sample that contained PEG polymers (as shown in FTICR MS) by size exclusion chromatography (SEC, Highload XK 16/60, Amersham Biosciences/GE Healthcare filled with Bio-Gel P-2 Gel, extra fine, Bio-Rad). Two fractions were extracted and lyophilized. The first one contained molecules in the 400–800 Da mass range (sample 1) and the second one contained substances of a molecular weight between 200 and 500 Da (sample 2). Their mass spectra are dominated by the polymer peaks observed as trains III (sample 1) and IV (sample 2) ionized by adducts of $NH_4^+$ (Fig. 10). PEG is easily ionized and causes an intense signal in MS measurements already at small concentration (0.2 $\mu$M) (Supplementary Fig. 1). In NMR measurements the signal

**Table 1** In the mass spectrum of one sample we find 12 different trains of peaks that originate from 12 different oligomers

| H+ | | M | Observed chain length | Possible linear structure formula | FTICR | | Q-Tof |
|---|---|---|---|---|---|---|---|
| | | | | | ESI | LDI | ESI |
| 371.23 | Train I | $C_{16}H_{34}O_9$ | 6 | $H\text{-}(C_2H_4O)_{m=8..14}\text{-}OH$ | x | x | |
| 335.28 | Train II | $C_{18}H_{38}O_5$ | 5 | $H\text{-}(CH_2)_{10}\text{-}(C_2H_4O)_{m=4..9}\text{-}OH$ | x | x | x |
| 349.29 | Train III | $C_{19}H_{40}O_5$ | 8 | $H\text{-}(CH_2)_{11}\text{-}(C_2H_4O)_{m=4..12}\text{-}OH$ | x | x | x |
| 319.28 | Train IV | $C_{18}H_{38}O_4$ | 7 | $H\text{-}(CH_2)_{12}\text{-}(C_2H_4O)_{m=3..10}\text{-}OH$ | x | x | x |
| 377.33 | Train V | $C_{21}H_{44}O_5$ | 1 | $H\text{-}(CH_2)_{13}\text{-}(C_2H_4O)_{m=4..5}\text{-}OH$ | x | | x |
| 391.31 | Train VI | $C_{21}H_{42}O_6$ | 1 | $(CH_2)_9\text{-}(C_2H_4O)_{m=6..7}$ | x | | x? |
| 349.15 | Train VII | $C_{10}H_{24}N_2O_{11}$ | 6 | $H\text{-}(CHOHO)_5\text{-}CH_2O\text{-}(CH_2NH)_2\text{-}(C_2H_4O)_{m=4..5}\text{-}H$ | | x | |
| 321.09 | Train VIII | $C_{11}H_{16}N_2O_9$ | 7 | | | x | x |
| 365.27 | Train IX | $C_{22}H_{36}O_4$ | 7 | | | x | x |
| 323.09 | Train X | $C_{14}H_{14}N_2O_7$ | 3 | | | x | x? |
| 377.18 | Train XI | $C_{12}H_{28}N_2O_{11}$ | 4 | | | x | x |
| 317.20 | Train XII | $C_{16}H_{28}O_6$ | 8 | | x | x | x |

All of them are composed of the same type of monomer. For each train, the mass of the shortest observed oligomer is given. High-resolution MS identified their molecular formula. The last columns state in which measurements the oligomers were found. Not all trains were found in all measurements. In a few cases the assignment to measurements with the Q-Tof is unsure due to its limited resolution (x?)

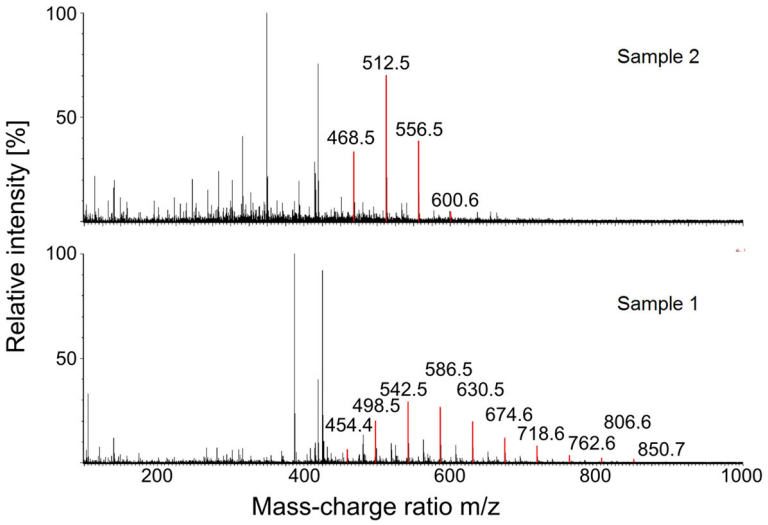


**Fig. 10** Mass spectra of the samples 1 and 2 of the SEC. The samples were lyophilized and prepared to be measured by NMR spectroscopy

intensity is proportional to the concentration of the substances. Therefore NMR measurements of the samples analyzed by ESI MS enables us to identify substances that are possibly suppressed in the MS measurement.

Both samples showed $^{1}$H resonances in the range 7.5–1 ppm, with the most intense signals between 3.6 to 1.1 ppm (corresponding to $^{13}$C in the range from 30 to 60 ppm, Fig. 11). Here we focus on the analysis of the most abundant components of the SEC purified samples, which lack aromatic moieties. In total nine $^{13}$C-$^{1}$H correlations could be identified, six of which were common to both samples (Table 2 and Supplementary Figs. 2–6). DQF-COSY and TOCSY spectra (Supplementary Figs. 2a and 4) revealed that moieties 2 and 3a/3b are coupled to each other through a $J_{HH}$ scalar coupling while moieties 5–7 are connected to 2–3 in a ROESY experiment, confirming that 2, 3, 5, 6 and 7 are part of the same molecule (Supplementary Figs. 2b and 5). The chemical shifts of this molecule are consistent with an alkane substituted with heteroatoms. Moieties 2 and 3a represent a -$CH_2$-$CH_2$- group which we attribute to an asymmetrically substituted 1, 2-diaminoethane. The singlet 3a can be assigned to a symmetrically substituted diaminoethane. The chemical shifts of moieties 5–7 are consistent with N-methyl groups. The relative intensities of resonances 2, 3, 5, 6 and 7, as well as the $^{13}$C chemical shifts differ slightly between samples 1 and 2 suggesting that these moieties are part of polymers with moderately different chemical composition. Their diffusion coefficients are in the range expected for a molecule of 200–500 Da for both samples (Supplementary Fig. 7). Taken together the data suggest the polymer of Fig. 12 as the probable major component of the SEC purified samples.

Sample 1 and 2 both contained moiety 1, which does not show correlations to other protons or carbons in any of the NMR spectra. Another isolated singlet was found only in sample 2 (moiety 8). Moiety 9, which is exclusive to sample 2 as well, correlates in the HMBC with a $^{13}$C resonance at 69.9 ppm. Carbon and hydrogen chemical shifts for this system are compatible with 2-methyl-2-propanol.

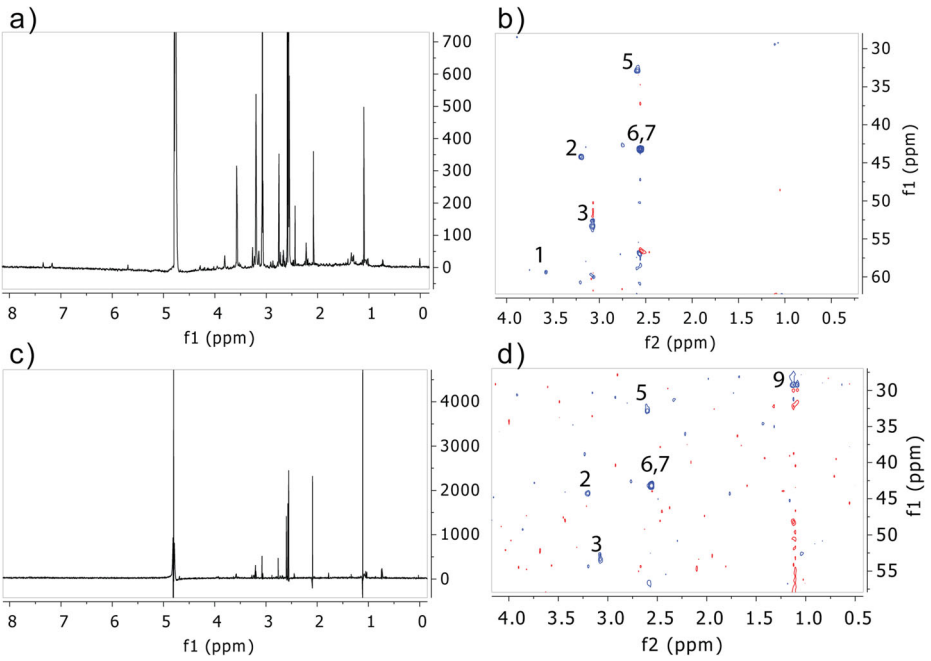


**Fig. 11** **a** $^{1}$H 1D full spectrum of sample 1, **b** $^{13}$C HMQC spectrum of sample 1, **c** $^{1}$H 1D full spectrum of sample 2, **d** $^{13}$C HMQC spectrum of sample 2. The numbers correspond to the spin systems as listed in Table 2

## Development of the pH Value

At the beginning of the experiments the solution was alkaline due to the dissolved ammonia (Fig. 13). During the first day the pH of the solution decreased continuously until it reached

**Table 2** Spin systems from the most abundant signals from the NMR measurements of sample 1 and 2

| Spin system | | Sample 1 | Sample 2 | Sample 1 | Sample 2 | |
|---|---|---|---|---|---|---|
| | $^{1}$H | $^{13}$C | $^{13}$C | I | I | M |
| 1 | 3.58 | 59.4 | | 0.3 | 1.3 | s |
| 2 | 3.20 | 44.2 | 44.0 | 1.0 | 1.0 | t: 6.6 |
| 3 | 3.07 | 52.6 | 53.4 | 2.0 | 1.3 | t: 6.6 |
| | | 53.4 | 52.7 | | | s |
| 5 | 2.59 | 32.9 | 32.9 | 1.4 | 1.0 | s |
| 6 | 2.56 | 43.2 | 43.2 | 2.9 | 1.0 | s |
| 7 | 2.57 | 43.2 | 43.2 | 2.8 | 1.9 | s |
| 8 | 2.09 | | | | 1.4 | s |
| 9 | 1.13 | | 29.3 | | 3.2 | s |

Moieties 8 and 9 were only present in sample 2. The chemical shifts from the $^{1}$H and $^{13}$C spectra (Fig. 11) are given. I, intensity of the peak normalized internally to I(2) = 1; M, multiplicity of the peak in the $^{1}$H 1D spectrum (s, singlet; t, triplet)

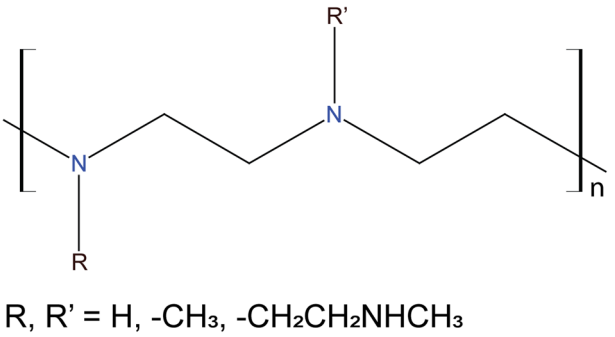


**Fig. 12** Schematic representation of the interpretation for the common signals of the NMR spectra from samples 1 and 2

a weakly acid value (pH 6.8). In other experiments we measured a neutral or weakly alkaline pH value (around pH 7.5) independent from the initial gas mixture.

## Discussion

We analyzed the mixture of the Miller-Urey experiment by different analytic techniques, sensitive to different chemical properties. Each technique highlights different molecular aspects.

The experiment produced thousands of molecules from a broad mass range. As already reported (Miller 1955) we observed traces of tungsten due to sputtering of the electrodes. We observed solid particles, however, our analysis focuses mainly on the soluble molecular fraction. ESI Q-Tof MS identified most substances from the aqueous solution within a distribution centered in vicinity of 300 Da (Fig. 2). The DBE and AI distributions (Fig. 5) are broad, suggesting substances from a wide degree of saturations and aromaticity. The extent of chemical variability is evidenced by the Van Krevelen diagrams. The produced substances cover many classes of organic molecules.

The Kendrick maps identified recurring $CH_2$ moieties as a common pattern, and NMR revealed alkanes as one of the most abundant species. Due to the low sensitivity of the ESI MS towards non-polarizable molecules as well as ionization competition we could not

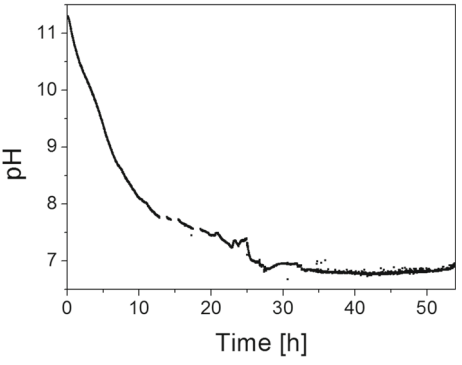


**Fig. 13** Continuous measurement of pH for an experiment in set-up I with a gas mixture of $CH_4$:$NH_3$:$H_2$ 1:1:0. From an alkaline state (about pH 11.3) the pH decreased until it reached a roughly constant value at about pH 6.8

detect pure alkanes in the high-resolution mass spectra. Instead, hydrocarbons with a large fraction of heteroatoms, aromatic and unsaturated substances including heteroatoms such as oxygen were prominent. We also detected alkane moieties attached to polar groups such as PEG or carboxylic groups.

From the Kendrick maps, HCN and NH moieties appeared as possible building blocks of the detected substances. Cyanides and C=N compounds may well result from reactions of HCN, produced in the discharge (Miller 1955). HCN is known to polymerize in multiple and complex ways. These different types of polymers have been studied in detail, exhibiting a large fraction of imines and amines (Bonnet et al. 2013; Matthews and Minard 2006; He et al. 2012). In the polymer fractions analyzed by NMR, amines were indeed the most abundant chemical group. This agrees well with the observation of amino acids (Miller 1955).

The Kendrick maps suggest CO groups as a common motif in the molecular structure. This may well reflect the existence of ketones and aldehydes as well as carboxylic and epoxy groups. We confirm the presence of aldehydes by MS/MS experiments that demonstrate the loss of formaldehyde ($CH_2O$) (Supplementary Table 2). A sufficiently large fraction of carboxylic groups is the likely reason for the strong decrease in the pH value over the first hours of the experiment. This is in agreement with the previous observations of organic acids (Miller 1953, 1955, 1957).

Ethers are easily ionized and polyethers can wrap protons and cations and this leads to a strong signal in the ESI MS measurements. However, PEGs were unstable in the mixture, they decayed within a day. Compared to MS the NMR measurements took orders of magnitude longer, of the order of a day, and PEG remained undetected in these measurements. PEG is stable in water and its decay is either due to ongoing chemical reactions after the end of the experiment or aggregation of PEG molecules that makes them hard to extract or to ionize.

In the initial gas mixture C and N were equally abundant whereas H was eight times more abundant. The amount of water as an oxygen source was largely above the amount of the gases, it mainly served as a solvent. In the gas phase the water concentration was around 2 mol/$m^3$ (gas phase saturated with water at an average temperature of roughly 35 °C). Taking the gas densities into account this leads to atomic ratios of roughly C:H:N:O 7:55:8:1. In the reactor new molecules were produced by the recombination of radicals and ions from the electric discharge. Since in the plasma, thermal energy is high compared to the ionization energies, naively, one could expect the atomic composition of the created substances to reflect the initial concentrations of the elements. Respecting chemical constraints this would lead to saturated molecules and a high atomic ratio of nitrogen. In the NMR measurements on fractions we find indeed a higher abundance of nitrogen than oxygen containing groups and aliphatic substances. High-resolution MS showed an (unweighted) average elemental composition of C:H:N:O of roughly 4:4:2:1 (exact 3.89:4.11:2.2:1.00). We conclude that chemical rules of composition are more important for the chemical mixture than relatively small variations in the initial concentrations of the gas mixture. This is in good agreement with the observations in Fig. 2. At the beginning of the experiment all substances were completely saturated, reactions between them necessarily lead to a decrease in the amount of hydrogen. Stability in water is another requirement.

Condensed aromatics, abundant in our mixture, are subject of the "aromatic world" hypothesis claiming that polycyclic aromatic hydrocarbons (PAH) played an important role at the origin of Life (Groen et al. 2012). They could have acted as pigments to drive chemical

reactions with photochemical energy. They are also suspected to catalyze the polymerization of biomolecules and to be able to build protocells (Menor-Salván et al. 2008; Ruiz-Mirazo et al. 2014; Groen et al. 2012). PAH has been suggested to have been brought to Earth by meteorites (Bernstein et al. 1999), however, our results suggest that PAH could have been produced endogenously given a sufficiently reducing atmosphere.

Due to our immediate analysis during the experiment, in a few samples we were able to observe short strands of PEG. Such strands are well known as organocatalysts (Totten and Clinton 1998; Anil Kumar et al. 2007). They can act through different mechanisms, among them template-based polymerization (Kim et al. 2003b). It is not clear how this polymer can form in the aqueous environment. In principle PEG can result from the condensation of ethanol. Ethanol is too small to be detected in our analysis but the presence of alcohols in the Miller-Urey experiment was reported before (Miller 1955, 1957). However, a polymerization reaction is not favored in water. PEG is usually synthesized by the polymerization of oxirane in organic solvents with small amounts of water and in the presence of a metal catalyst (Starks et al. 1994; Kiesewetter et al. 2010). Synthesis with organic catalysts has been reported as well, however, not in the presence of water. (Kiesewetter et al. 2010; Yang and Ting 1993). Reactions that reverse hydrolysis belong to the riddles of the origin of Life, and this needs to be investigated further (Ruiz-Mirazo et al. 2014). The polymerization reaction of HCN yields a large variety of nitrogen-rich polymers (Matthews 1975; Ferris and Hagan 1984; Matthews and Minard 2006; Bonnet et al. 2013; He et al. 2012). Nucleic acid bases and amino acids can be among them (Ruiz-Bermejo et al. 2012). HCN polymers were discussed to play a possible role as condensation agents, as well as photocatalysts in prebiotic chemistry (Ferris and Hagan 1984; Wang et al. 2009; Ruiz-Bermejo et al. 2012). Stanley Miller reported the synthesis of nitrogen and oxygen containing polymeric compounds on the electrodes of his experiment (Miller 1955, 1957).

The application of different analytical techniques to the mixture of the Miller-Urey experiment revealed a large number of substances, among them organocatalysts. As far as we can say from our global approach, these species are not mere side products of a few preferred products. Rather many different species appear with equally important concentrations. In view of the simplicity of our setup, this comes as surprise. The reaction dynamics of this mixture could certainly become very complex upon energetic driving. Organic catalysts that appear in the broth may well lead to the production of molecular species that would normally not be favored under the conditions in the reactor, further enhancing the molecular richness. The suspected reversal of hydrolysis, required for the formation of PEG, points towards the presence of such unidentified organocatalysts of unknown nature.

In a second contribution we will focus on more hydrophobic substances, presenting results from gas chromatography, mass spectrometry, NMR and coherent anti-Stokes Raman spectroscopy (CARS). In further studies we plan to address the question of how the molecular complexity builds up and how it may reflect back to the reaction network.

**Acknowledgments** We thank Karsten Kruse, Uli Kazmaier, Gerhard Wenz, Michael Veith, Josef Zapp, Hermann Sachdev, Daniel Krug and the Department of Pharmaceutical Biotechnology, Reiner Wintringer and the Institute for Bioanalytical Chemistry and Klaus Schappert. We thank Jörg Schmauch for contributing the SEM measurements and the EDS analysis.

Financial support from the National FT-ICR network (FR 3624 CNRS) for conducting the research is gratefully acknowledged.

## References


Anil Kumar M, Stephen Babu M, Srinivasulu K, Kiran Y, Suresh Reddy C (2007) Polyethylene glycol in water: A simple and environment friendly media for Strecker reaction. J Mol Catal A-Chem 265:268–271

Bax A, Summers M (1986) Proton and carbon-13 assignments from sensitivity-enhanced detection of heteronuclear multiple-bond connectivity by 2D multiple quantum NMR. J Am Chem Soc 108:2093–2094

Bax A, Griffey R, Hawkins B (1983) Correlation of proton and nitrogen-15 chemical shifts by multiple quantum NMR. J Magn Reson 55:301–315

Bernstein MP, Sandford SA, Allamandola LJ, Gillette JS, Clemett SJ, Zare RN (1999) UV irradiation of polycyclic aromatic hydrocarbons in ices: Production of alcohols, quinones, and ethers. Science 283:1135–1138

Bonnet JY, Thissen R, Frisari M, Vuitton V, Quirico E, Orthous-Daunay FR, Dutuit O, Le Roy L, Fray N, Cottin H, Hörst SM, Yelle R (2013) Compositional and structural investigation of HCN polymer through high resolution mass spectrometry. Int J Mass Spectrom 354-355:193–203

Bothner-By AA, Stephens RL, Lee J, Warren CD, Jeanloz RW (1984) Structure determination of a tetrasaccharide: transient nuclear Overhauser effects in the rotating frame. J Am Chem Soc 106:811–813

Braunschweiler L, Ernst R (1983) Coherence transfer by isotropic mixing: application to proton correlation spectroscopy. J Magn Reson 53:521–528

Cleaves HJ, Chalmers JH, Lazcano A, Miller SL, Bada JL (2008) A reassessment of prebiotic organic synthesis in neutral planetary atmospheres. Orig Life Evol Biosph 38:105–115

Ferris JP, Hagan WJ (1984) HCN and chemical evolution: The possible role of cyano compounds in prebiotic sythesis. Tetrahedron 40:1093–1120

Ferus M, Nesvornýc D, Šponer J, Kubelíka P, Michalčíková R, Shestivská V, Šponer J, Civiš S (2014) High-energy chemistry of formamide: A unified mechanism of nucleobase formation. Proc Natl Acad Sci 112:657–662

Fox SW (1995) Thermal synthesis of amino acids and the origin of life. Geochim Cosmochim Acta 59:1213–1214

Greig M, Griffey RH (1995) Utility of organic bases for improved electrospray mass spectrometry of oligonucleotides. Rapid Commun Mass Spectrom 9:97–102

Groen J, Deamer DW, Kros A, Ehrenfreund P (2012) Polycyclic aromatic hydrocarbons as plausible prebiotic membrane components. Orig Life Evol Biosph 42:295–306

Gross JH (2011) Mass spectrometry: a textbook. Springer, Berlin

He C, Guangxin L, Upton KT, Imanaka H, Smith MA (2012) Structural investigation of HCN polymer isotopomers by solution-state multidimensional NMR. J Phys Chem A 116:4751–4759

Hertkorn N, Frommberger M, Witt M, Koch BP, Schmitt-Kopplin P, Perdue EM (2008) Natural organic matter and the event horizon of mass spectrometry. Anal Chem 80:8908–8919

Johnson AP, Cleaves HJ, Dworkin JP, Glavin DP, Lazcano A, Bada JL (2008) The Miller volcanic spark discharge experiment. Science 322:404–404

Kalinoski HT, Hargiss LO (1992) Collision-induced dissociation mass spectrometry of nonionic surfactants following direct supercritical fluid injection. J Am Soc Mass Spectrom 3:150–158

Kendrick E (1963) A mass scale based on $CH_2 = 14.0000$ for high resolution mass spectrometry of organic compounds. Anal Chem 35:2146–2154

Kiesewetter M, Shin E, Hedrick J (2010) Organocatalysis: opportunities and challenges for polymer synthesis. Macromolecules 43:2093–2107

Kim S, Kramer RW, Hatcher PG (2003a) Graphical method for analysis of ultrahigh-resolution broadband mass spectra of natural organic matter, the Van Krevelen diagram. Anal Chem 75:5336–5344

Kim YJ, Uyama H, Kobayashi S (2003b) Regioselective synthesis of poly(phenylene) as a complex with poly(ethylene glycol) by template polymerization of phenol in water. Macromolecules 36:5058–5060

Kobayashi K, Kaneko T, Saito T, Oshima T (1998) Amino acid formation in gas mixtures by high energy particle irradiation. Orig Life Evol Biosph 28:155–165

Koch BP, Dittmar T (2006) From mass to structure: an aromaticity index for high-resolution mass data of natural organic matter. Rapid Commun Mass Spectrom 20:926–932

Lattimer RP (1992a) Tandem mass spectrometry of lithium-attachment ions from polyglycols. J Am Soc Mass Spectrom 3:225–234

Lattimer RP (1992b) Tandem mass spectrometry of poly(ethylene glycol) proton- and deuteron-attachment ions. Int J Mass Spectrom Ion Process 116:23–26

Lowe CU, Rees MW, Markham R (1963) Synthesis of complex organic compounds from simple precursors: formation of amino-acids, amino-acid polymers, fatty acids and purines from ammonium cyanide. Nature 199:219–222

Matthews CN (1975) The origin of proteins: Heteropolypeptides from hydrogen cyanide and water. Orig Life 6:155–162

Matthews CN, Minard RD (2006) Hydrogen cyanide polymers, comets and the origin of life. Faraday Discuss 133:393–401

McCollom TM, Ritter G, Simoneit BRT (1999) Lipid synthesis under hydrothermal conditions by fischer-tropsch-type reactions. Orig Life Evol Biosph 29:153–166

Menor-Salván C, Ruiz-Bermejo M, Osuna-Esteban S, Muñoz-Caro G, Veintemillas-Verdaguer S (2008) Synthesis of polycyclic aromatic hydrocarbons and acetylene polymers in ice: a prebiotic scenario. Chem Biodivers 5:2729–2739

Miller SL (1953) A production of amino acids under possible primitive earth conditions. Science 117:528–529

Miller SL (1955) Production of some organic compounds under possible primitive earth conditions. J Am Chem Soc 77:2351–2361

Miller SL (1957) The mechanism of synthesis of amino acids by electric discharges. Biochim Biophys Acta 23:490–498

Miyakawa S, Yamanashi H, Kobayashi K, Cleaves HJ, Miller SL (2002) Prebiotic synthesis from CO atmospheres: implications for the origins of life. Proc Natl Acad Sci 99:14,628–14,631

Oró J (1960) Synthesis of adenine from ammonium cyanide. Biochem Biophys Res Comm 2:407–412

Oró J (1961) Mechanism of synthesis of adenine from hydrogen cyanide under possible primitive earth conditions. Nature 191:1193–1194

Oró J (1963) Synthesis of organic compounds by electric discharge. Nature 197:862–867

Oró J, Kimball A, Fritz R, Master F (1959) Amino acid synthesis from formaldehyde and hydroxylamine. Arch Biochem Biophys 86:115–130

Parker ET, Cleaves HJ, Dworkin JP, Glavin DP, Callahan M, Aubrey A, Lazcano A, Bada JL (2011) Primordial synthesis of amines and amino acids in a 1958 Miller $H_2S$-rich spark discharge experiment. Proc Natl Acad Sci 108:5526–5531

Piantini U, Sorensen OW, Ernst RR (1982) Multiple quantum filters for elucidating NMR coupling networks. J Am Chem Soc 104:6800–6801

Reemtsma T (2009) Determination of molecular formulas of natural organic matter molecules by (ultra-) high-resolution mass spectrometry: Status and needs. J Chromatogr A 1216:3687–3701

Ruiz-Bermejo M, de la Fuente JL, Rogero C, Menor-Salván C, Osuna-Esteban S, Martìn-Gago J (2012) New insights into the characterization of insoluble black HCN polymers. Chem Biodivers 9:25–40

Ruiz-Mirazo K, Briones C, de la Escosura A (2014) Prebiotic systems chemistry: New perspectives for the origins of life. Chem Rev 114:285–366

Sanchez R, Ferris J, Orgel LE (1966a) Conditions for purine synthesis: Did prebiotic synthesis occur at low temperatures? Science 153:72–73

Sanchez R, Ferris J, Orgel LE (1966b) Cyanoacetylene in prebiotic synthesis. Science 154:784–785

Santamaria L, Fleischmann L (1966) Photochemical synthesis of amino acids from paraformaldehyde catalysed by inorganic agents. Experientia 22:430–431

Schlesinger G, Miller SL (1983) Prebiotic synthesis in atmospheres containing $CH_4$, CO, and $CO_2$. J Mol Evol 19:376–382

Schramm S, Carré V, Scheffler JL, Aubriet F (2011) Analysis of mainstream and sidestream cigarette smoke particulate matter by laser desorption mass spectrometry. Anal Chem 83:133–142

Selby TL, Wesdemiotis C, Lattimer RP (1994) Dissociation characteristics of [M + X]+ ions (X = H, Li, Na, K) from linear and cyclic polyglycols. Int J Mass Spectrom Ion Process 5:1081–1092

Shaw GH (2008) Earth's atmosphere - hadean to early proterozoic. Chem Erde 68:235–264

Simionescu CI, Totolin MI, Denes F (1976) Abiotic synthesis of some polysaccharide-like and polypeptide-like structures in cold plasma. Biosystems 8:153–158

Starks CM, Liotta CL, Halpern ME (1994) Phase-transfer catalysis–fundamentals, applications and industrial perspectives. Springer-Science+Business Media, Dordrecht

Tian F, Kasting J, Zahnle K (2011) Revisiting HCN formation in earth's early atmosphere. Earth Planet Sci Lett 308:417–423

Totten GE, Clinton NA (1998) Poly(ethylene glycol) and derivatives as phase transfer catalysts. J Macromol Sci-Pol R 38:77–142

Trinks H, Schröder W, Biebricher CK (2005) Ice and the origin of life. Orig Life Evol Biosph 35:429–445

Wang X, Maeda K, Chen X, Takanabe K, Domen K, Hou Y, Fu X, Antonietti M (2009) Polymer semiconductors for artificial photosynthesis: Hydrogen evolution by mesoporous graphitic carbon nitride with visible light. J Am Chem Soc 131:1680–1681

Watson JT, Sparkman OD (2008) Introduction to mass spectrometry: Instrumentation, applications and strategies for data interpretation. Wiley, Chichester

Willcott MR (2009) MestRe Nova. J Am Chem Soc 131:13,180–13,180

Wu D, Chen A, Johnson C (1995) An improved diffusion-ordered spectroscopy experiment incorporating bipolar-gradient pulses. J Magn Reson A 115:260–264

Yang CP, Ting CY (1993) Preparation of quaternary ammonium resin by epoxy resin and tertiary amine and its electrodeposition properties. J Appl Polym Sci 49:1019–1029